Journal of Molecular Liquids 335 (2021) 116178

Contents lists available at ScienceDirect

Journal of Molecular Liquids

journal homepage: www.elsevier.com/locate/molliq

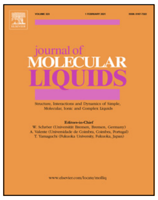

Synthesis and mesomorphic properties of bis ester derivatives of coumarin containing chalcone linkage

Priyanka Shah [1], Rina Soni [1], Shubhangi S Soman *

Department of Chemistry, Faculty of Science, The M. S. University of Baroda, Vadodara 390 002, India

ARTICLE INFO

Article history:
Received 17 December 2020
Revised 27 March 2021
Accepted 13 April 2021
Available online 17 April 2021

Keywords:
Coumarin
Bis ester
Chalcone
Mesomorphic
Photophysical

ABSTRACT

Bis ester derivatives of coumarin containing chalcone linkage with various terminal alkoxy groups were designed, synthesized and characterized. Compounds **11a-m** were studied for their mesomorphic properties using polarizing optical microscope & differential scanning calorimetry and photophysical properties using UV-vis & fluorescence spectroscopy. In this particular homologous series, compounds having lower flexible alkoxy chains showed very good mesogenic property with nematic mesophase formation, while analogues with higher chains failed to show any liquid crystalline property. Compound **11a** with methoxy group showed very good absorbance and fluorescence as compared to higher chain length analogues.

© 2021 Elsevier B.V. All rights reserved.

1. Introduction

Thermotropic liquid crystalline compounds containing heterocyclic ring is developing area of research in liquid crystalline material [1–5]. Thermotropic liquid crystalline materials with nematic mesophase are important due to their large temperature range and they have been used in liquid crystal displays. The type of mesophase and layer arrangement can be affected by small changes in the molecular shape in thermotropic rod shape liquid crystalline molecules. At the same time central linkage plays important role not only in formation of mesophase but also in thermal stability and temperature range of mesophase [6–10]

Coumarin is one of the interesting heterocyclic ring which can enhance all required properties in liquid crystalline material including photoluminescence due to its very good photophysical nature. Coumarins absorption and emission wavelength and photoluminescence properties strongly depend on the nature and the position of substituents [11]. Coumarin derivatives are well explored for optical data storage materials as they have good solubility in organic solvents along with very good photostability and high quantum yield [12–14]. Moreover, the relative ease of synthesis and high solubility make them suitable materials for optoelectronic devices [15–17]. Coumarin containing thermotropic liquid crystal compounds are reported for their mesomorphic properties [18–21].

Recently, Mohammad *et al* synthesized three new homologous series of coumarin heterocycles-derived symmetric dimers **1** containing two Schiff base moieties as connected by phenyl ring (Fig. 1) [22]. These synthesised compounds with terminal alkyl chain above ten carbon length exhibited liquid crystalline properties, while compounds with lower alkyl chains are hard to exhibit mesophase. Same group has also reported coumarin substituted symmetric diaminopyridine molecules **2** as thermotropic liquid crystals [23]. In this particular series of compound **2** with short chains were found to be not showing any mesophase whereas compounds with long-chains exhibited nematic mesophase only.

Ngaini & Hegde et al have reported azobenzene substituted coumarin derivatives **3** bearing different alkoxy chains for their liquid crystalline properties and photo switching properties (Fig. 1) [24]. Azo-coumarin compound 3 with alkyl chain C6 to C12 showed nematic phase while with C14 alkyl chain exhibited Smectic–A phase.

Our group had reported coumarin derivatives with chalcone **4** and imine **5** linkages and studied their mesomorphic properties (Fig. 1). Coumarin derivatives with chalcone linkage showed mesomorphic property with terminal alkyl chain hexyl and above [25]. Schiff base linkages containing coumarin derivatives **5** exhibited mesomorphic behaviour from propyloxy chain onwards. As a part of further modification in coumarin chalcone derivatives we have replaced terminal alkoxy group by ester to study their mesomorphic property. Herein we report synthesis and mesomorphic

---

* Corresponding author.
E-mail address: shubhangiss@rediffmail.com (S.S Soman).

[1] Both the authors have contributed equally.

https://doi.org/10.1016/j.molliq.2021.116178
0167-7322/© 2021 Elsevier B.V. All rights reserved.

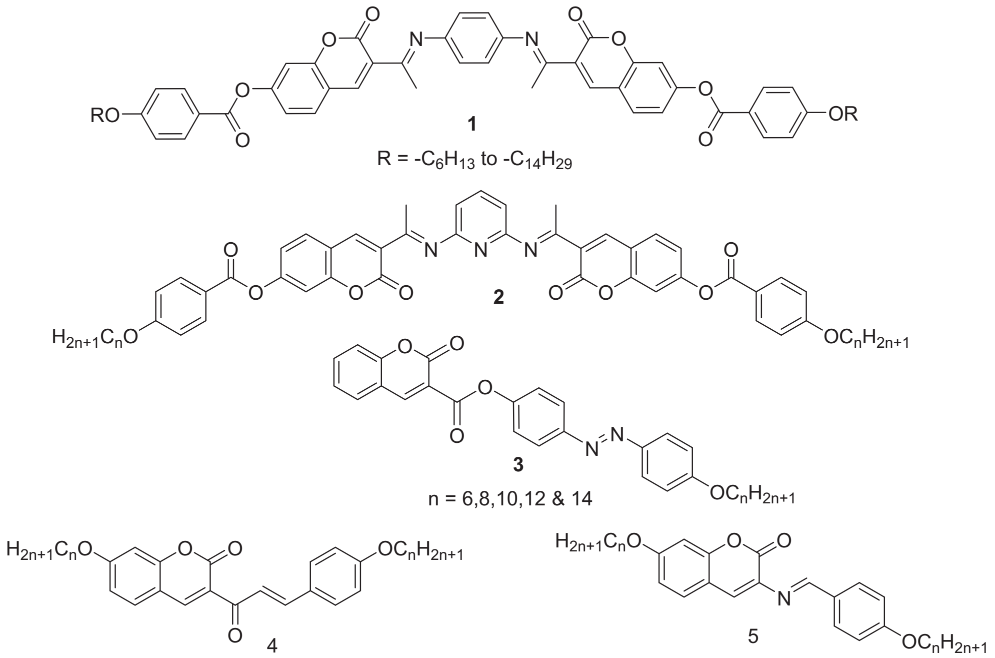

Fig. 1. Coumarin derivatives with liquid crystalline properties.

properties of bis ester derivatives of coumarin containing chalcone linkage. The mesomorphic behaviour of the homologous compounds with chalcone linkage with varying length of the terminal alkyl chains were studied along with their photophysical properties.

2. Results and discussion

2.1. Chemistry

Compound **11a-m** were prepared in two steps from 3-acetyl-7-hydroxy-chromen-2-one **8** (Scheme 1). Compound **8** was reacted with 4-hydroxy benzaldehyde in ethanol using catalytic amount of piperidine and acetic acid to give compound **10**. Compound **10** was esterified with 4-alkoxy benzoic acid **7a-m** using EDC, HOBt and TEA in DCM to give compound **11a-m** (Scheme 1). All synthesized compounds were analysed by different analytical techniques such as ^{1}H- NMR, ^{13}C NMR and IR analysis to confirm their structures.

IR spectrum of the compound **11d** showed broad peaks in the region of 2956–2870 cm^{-1} for alkyl chain C-H stretching, at 1727 cm^{-1} for carbonyl stretching of lactone ring along with ester and at 1659 cm^{-1} for carbonyl stretching of chalcone. ^{1}H NMR of compound **11d** showed peaks corresponding to methyl and methy-

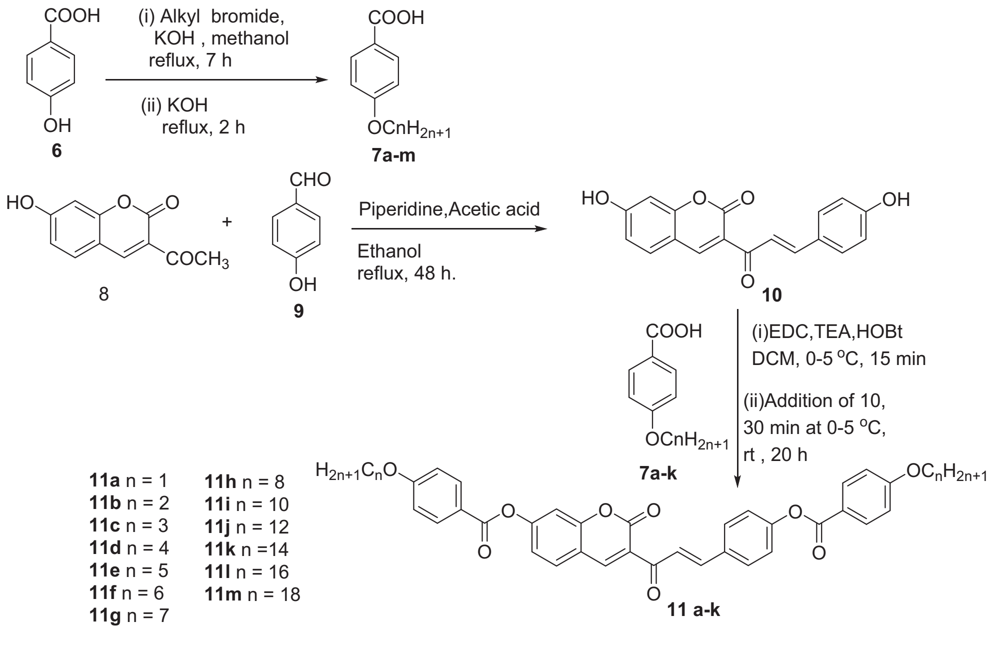

Scheme 1. Synthesis of coumarin bis ester derivatives with chalcone linkage.

Table 1
Phase assignments, transition temperature °C of compounds **11a-m** as determined by POM and DSC.

Compd	Chain length	2nd heating process^{a} (onset 10 °C/min) [°C]/[ΔH KJmol^{-1}]	1st cooling process^{a} (onset 10 °C/min) [°C]/[ΔH KJmol^{-1}]
11a	1	Cr 176.39(34.22) Iso	Iso Cr ^{b}
11b	2	Cr 173.93(44.11) Iso	Iso 144.52(21.90) Cr
11c	3	Cr 180.21^{c} N 184.61(29.38) Iso	Iso N^{d} 163.94(19.52) Cr
11d	4	Cr 187.14^{c} N 193.18(30.94) Iso	Iso N^{d} 164.73(14.68) Cr
11e	5	Cr 181.73(35.81) N 196.58 (0.62) Iso	Iso N^{d} 141.63(11.18) Cr
11f	6	Cr 179.34(36.63) N 198.19 (1.03) Iso	Iso 144.99(0.31) N 135.07 (5.74) Cr
11g	7	Cr 176.32(38.03) N 193.70 (0.65) Iso	Iso 151.81(2.14) N 102.49 (4.89) Cr
11h	8	Cr 168.23(21.22) Cr1 180.33(1.21) Iso	Iso 145.90(3.15) Cr
11i	10	Cr 156.98(23.80) Cr1 182.32(4.90) Iso	Iso 157.07(3.03) Cr
11j	12	Cr 145.84(24.06) Cr1 189.97(2.38) Iso	Iso 192.58(5.98) Cr
11k	14	Cr 95.65(34.18) Cr1 178.11 (3.96) Iso	Iso 171.18(4.82) Cr
11l	16	Cr 98.03(17.81) Cr1 186.83 (6.81) Iso	Iso 175.09(3.99) Cr
11*m*	18	Cr 98.23(23.80) Cr1 168.70 (0.99) Iso	Iso 154.08 (1.97) Cr

[a] Cr: Crystalline state; N: Nematic phase; I: Isotropic state, Cr/Cr1: crystal to crystal transition

[b] Temperature for crystallization was not obtained in DSC thermogram.

[c] Mesophase transition during heating cycle has merged with peak observed for isotropic phase transition in DSC thermogram.

[d] Mesophase transition during cooling cycle has merged with peak observed for crystallization phase transition DSC thermogram.

lene groups in the region of 1.02–1.87 ppm and methylene groups in region of 1.02–1.87 ppm and methylene groups bearing oxygen were observed in region of 4.06–4.10. Aromatic protons were observed in region of 7.00–8.64 ppm along with chalcone protons as doublet at 7.90 and 7.95 with coupling constant value of 16.0 Hz indicated trans coupling. ^{13}C NMR of the compound **11d** showed peaks for methyl and methylene carbons from 13.85 to 68.13 ppm, aromatic carbons appeared from 110.4 to 164.57 ppm along with carbonyl carbon of ester and lactone group and carbonyl carbon of chalcone were appeared at 186.13 ppm.

2.2. Mesomorphic properties

2.2.1. Differential scanning calorimetry study (DSC)

Compounds **11a-m** were studied for phase identification and optical textures using polarizing optical microscope. Mesophase transition temperatures were further confirmed by differential scanning calorimetry (DSC). For phase identification using POM, thin film of compound was placed on glass slide, covered with cover slip and heated at the rate of 10 °C/min to give isotropic liquid. Changes in textures were observed under microscope under 1st cooling cycle and 2nd heating cycle at the rate of 10 °C/min. Thermograms were calculated by DSC (DSC-822, Mettler Toledo having Stare software) in heating and cooling cycle at the rate of 10 °C/min. Clear-cut transition temperatures and textures could be obtained from DSC curves and POM observations for all of the compounds, and they were in good agreement with each other for the multiple heating/cooling cycles (Table 1).

Bis ester derivative of coumarin compound **11a** showed one endotherm for crystalline to Isotopic phase (Cry-Iso), however any exotherm was not observed during cooling cycle. Compound **11b** showed one endotherm for crystalline to Isotropic phase (Cr-Iso) in heating cycle and one exotherm during cooling cycle for isotropic to crystallization (Iso-Cr). Compound **11c** showed two endotherms for crystalline to nematic phase (Cr-N) and nematic to isotropic phase (N-Iso), however only one exotherm was observed during cooling cycle. Compounds **11b** and **11d** with ethyl and butyl side chains showed one endotherm for crystalline to isotropic liquid phase on heating and one exotherm from isotropic liquid phase to crystallization (Iso-Cr) on cooling. Compound **11e** exhibited two endotherms from crystalline solid to nematic phase (Cr-N) and nematic phase to isotropic liquid phase (N-Iso) on heating, while on cooling only one exotherm was observed corresponding to isotropic liquid phase to crystalline solid state (Iso-Cr). Compounds **11f** and **11g** showed two endotherms for heating cycle and two exotherms on cooling cycle, while heating first transition was observed from crystalline solid to nematic mesophase (Cr-N), second transition was observed for nematic phase to isotropic liquid phase (N-Iso) (Fig. 2a-b). Isotropic liquid phase to nematic phase (Iso-N), nematic to crystalline solid (N-Cr) for compounds **11f** and **11g** was observed in cooling cycle as shown in (Fig. 2a-b, Table 1). Compounds **11h** with octyloxy side chain showed only two endotherms during heating cycle for crystalline to crystalline 1 transition (Cr-Cr1) at lower temperature and crystalline 1 to isotropic liquid phase (Cr1-Iso) and one exotherm observed during cooling cycle (Table 1). All higher analogues in this series with decyloxy to octadecyloxy side chains, compounds **11i-m** showed two endotherms in heating cycle corresponding crystalline to crystalline 1 transition (Cr-Cr1) at lower temperature and crystalline 1 to isotropic liquid phase (Cr1-Iso). In cooling cycles, compounds **11i-m** showed one exotherm corresponding to isotropic liquid phase to crystalline solid (Iso-Cr) (Table 1).

2.2.2. Polarising optical microscopy (POM) study

Liquid crystal phase transitions for compounds **11a-m** were studied using polarizing optical microscope. Thin film of compound was prepared by heating small amount of compound sandwiched between glass slide and cover slip and heated at the rate of 10 °C/min. Changes in textures were observed under microscope under 1st cooling cycle and 2nd heating cycle at the rate of 10 °C/min.

Liquid crystal phase transitions for compound **11c** with propyloxy group are illustrated in Fig. 3. By bringing the temperature up to 180.21 °C at the rate of 10 °C/min, crystalline to nematic droplet transition was observed. On further heating up to 184.61 °C, the nematic phase lost its birefringence and was transformed to an isotropic phase. By cooling the isotropic phase at 10 °C/min, nematic droplets began to appear (Fig. 3a) and coalesce forming a nematic marble texture (Fig. 3b). The nematic marble texture was changed to crystalline solid when temperature is reduced to 163.94 °C.

In heating scan at the rate of 10 °C/min, compound **11d** with butyloxy side chain showed nematic texture at 187.14 °C and turned to isotropic liquid on heating up to 193.18 °C. In cooling scan at the rate of 10 °C/min, compound **11d** showed neamtic marble texture (Fig. 3c), which was changed to nematic schlieren texture (Fig. 3d) on cooling followed by nematic phase lost its birefringence and was transformed into crystalline solid when temperature is reduced to 164.73 °C.

On changing the chain length from butyloxy to pentyloxy group in compounds **11e** showed nematic transitions during heating cycle at 181.73 °C (Fig. 4a). On changing the chain length from pentyloxy to hexyloxy group in compounds **11f** showed nematic transitions during heating and cooling cycles (Fig. 4b). Similarly, compound **11g** showed nematic phase at 176.32 °C (Fig. 4c) which on further heating up to 193.70 °C, the nematic phase lost its birefringence and was transformed to an isotropic phase. In cooling scan at 10 °C/min for compound **11g**, nematic marble texture appeared at 151.81 °C (Fig. 4d). On further cooling, this nematic

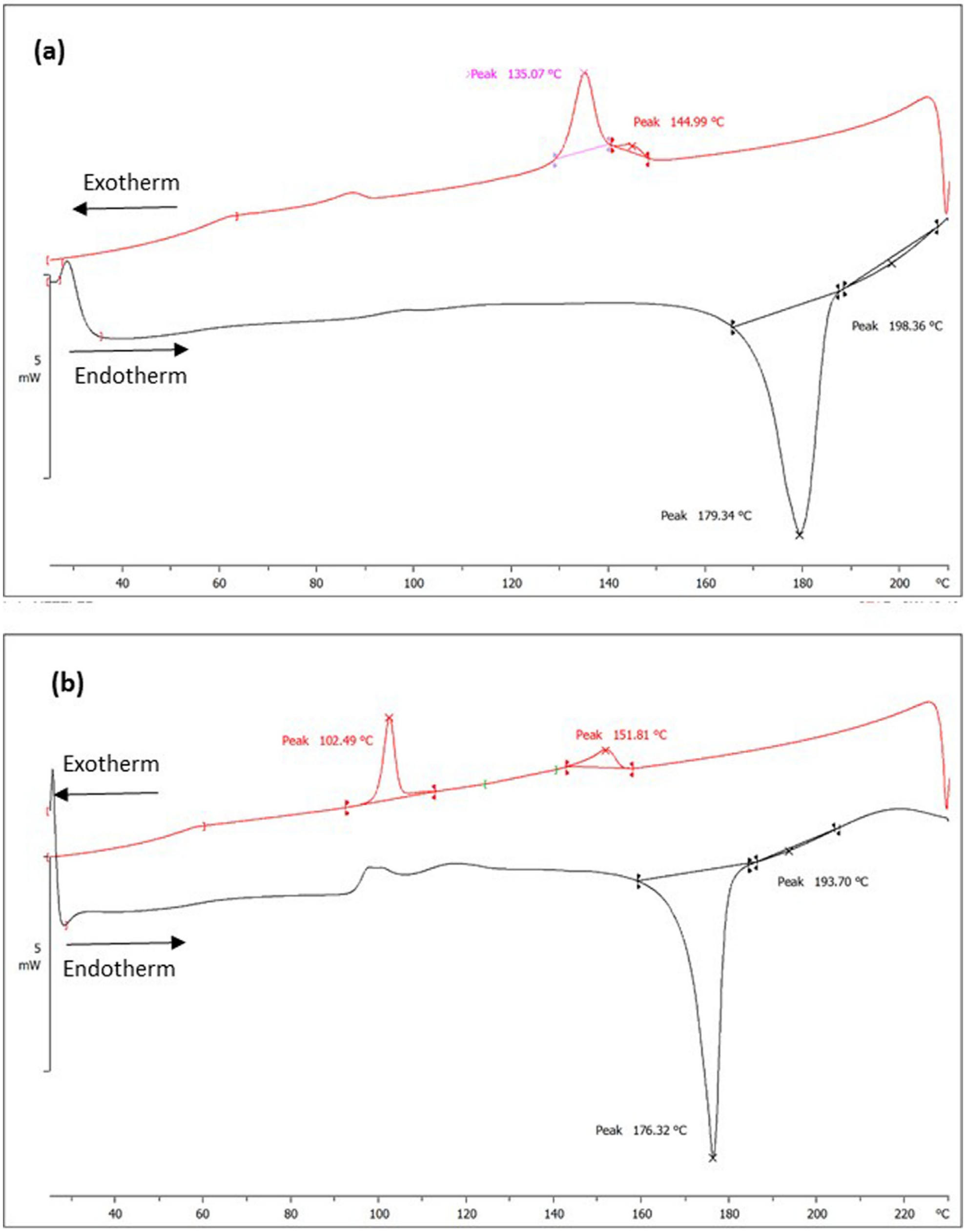

Fig. 2. a-**d.** DSC plots in both heating and cooling cycles along with transition temperatures (a) compound **11f** with hexyloxy chain (b) compound **11g** with heptyloxy chain.

texture was changed to crystalline solid at 102.49 °C. Compounds **11h-m** with alkoxy chain of C8, C10, C12, C14, C16 and C18 respectively, were crystallized without showing any mesophase transition during 1st cooling cycle (Fig. 5a-b). Similarly in 2nd heating cycle, compounds **11h-m** were converted directly to isotopic liquid without showing any mesophase transition.

2.3. Structure-mesomorphic property relationship

The graph of phase-transition temperatures against the number of carbons in bis-ester derivatives of coumarin containing chalcone linkage with various *n*-alkoxy chains enabled the effects of the terminal chain on the mesomorphic properties. The relationship was established from two different plots (Fig. 6). The Cr-N/Iso transition curve exhibited sharp increase tendency with the melting temperatures increased from ethyloxy derivative **11b** to hexyloxy derivative **11f** and covers large area which may be responsible for the enantiotropy nature of the series. From compounds **11g** to **11m** zig-zag trend was observed as alkyl chains are increased in both the terminal and these may lead to the excessive Van der Waals attractive forces between the long alkyl chains. Compounds **11c-11g** showed N-Iso transition, initially it has increased from propyloxy to butyloxy side chain and then falling tendency from butyloxy to heptyloxy side chain. In cooling cycle, the Iso-N transition curve was obtained for only two compounds **11f** and **11g** which showed increasing tendency, however lower members of these series showed nematic mesophase in POM study but transition phases were not observed in DSC thermograms. In literature, long chain bis esters have shown mesomorphic properties [22,23], however higher members of this series with octyloxy chain onwards, failed to show any mesophase. The low melting points and excessive Van der Waals attractive forces of these higher members of series may be partially responsible for the lack of mesophase formation. The exotherms observed for these compounds during

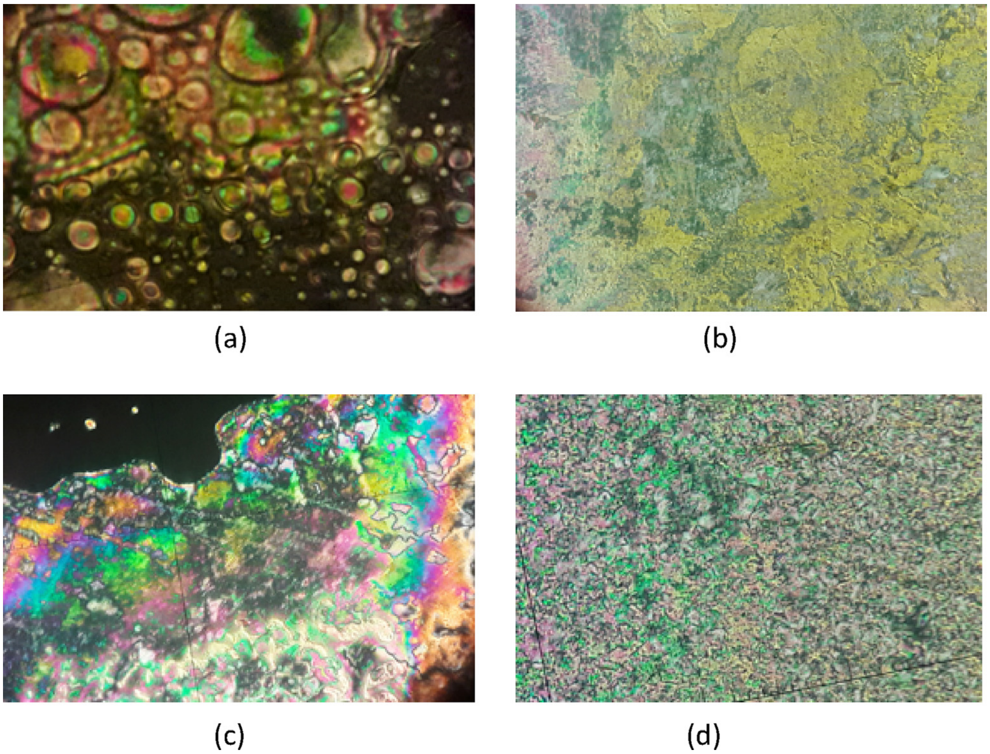

Fig. 3. a-d. Liquid crystal phase transition for compound **11c** (a) nematic droplet (b) nematic marble texture; for compound **11d** (c) nematic marble texture (d) nematic schlieren texture.

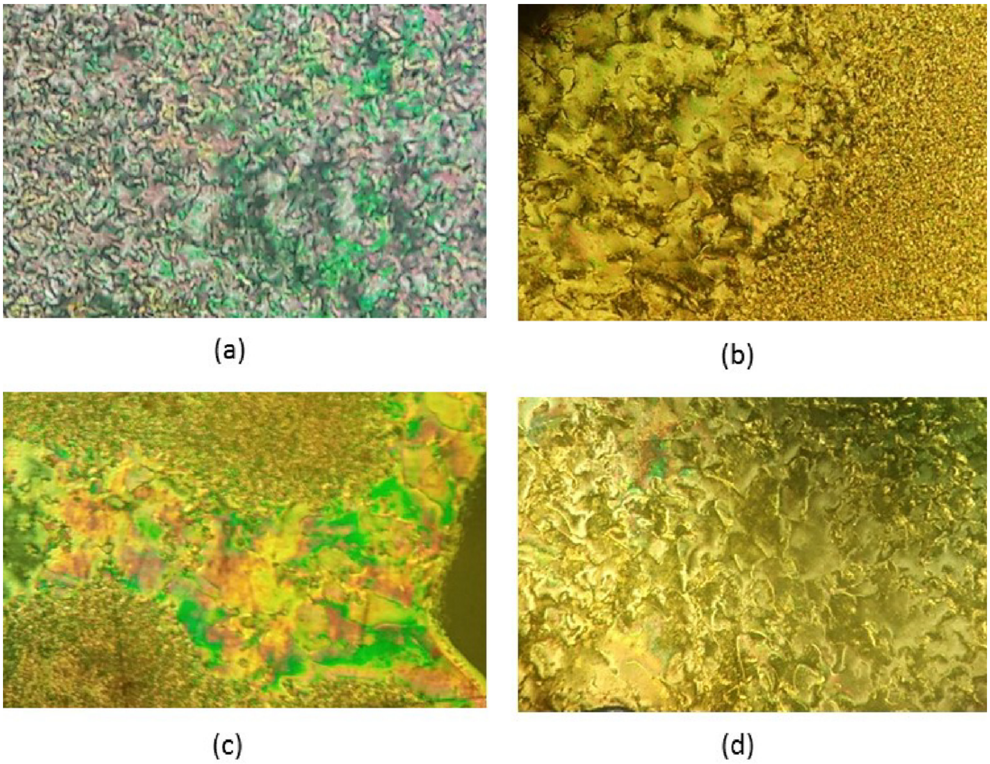

Fig. 4. a-d. Liquid crystal phase transition (a) compound **11e** nematic schlieren texture (b) compound **11f** nematic schlieren texture (c) compound **11g** nematic marble texture in heating (d) compound **11g** nematic marble texture in cooling.

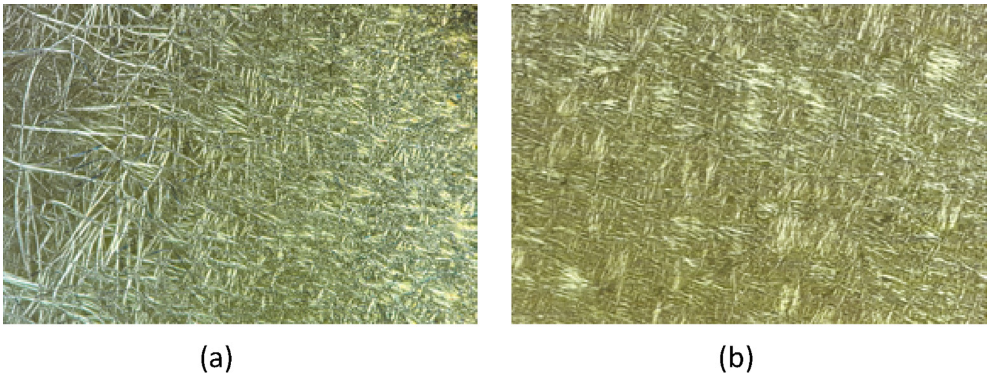

Fig. 5. **a-b.** Liquid crystal phase transition analysis giving direct crystallization (a) compound **11h** (b) compound **11i**.

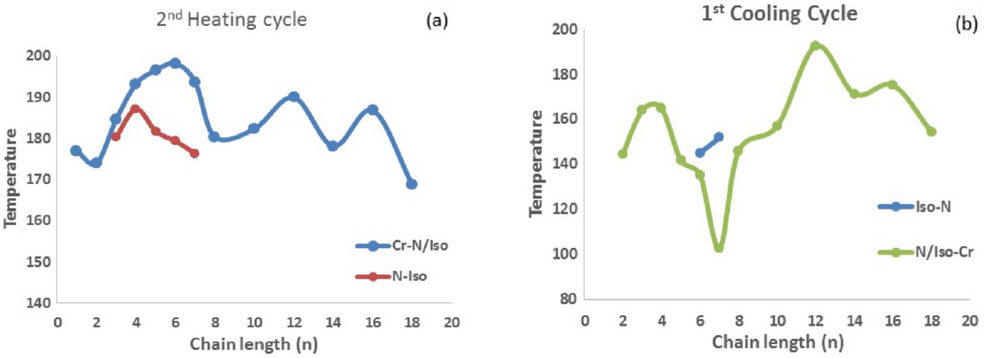

Fig. 6. Mesomorphic behaviour as a function of the number of carbon atoms (n) in the terminal alkoxy chain (a) 2nd in heating cycle (b) in 1st cooling cycle.

cooling cycle in DSC analysis have shown similar trend and supported non-existence of mesomorphic properties. The odd-even effect was not very much clear in this particular series in both heating and cooling cycles may be due to sequential increase of chain lengths at the both sides of molecule, which has resulted in excessive Van der Waals attractive forces and compounds were found to be greasy in nature.

2.4. Photophysical properties

A photophysical study of the coumarin derivatives **11a-m** was performed to evaluate their absorption and emission spectra in solutions of chloroform at room temperature. Fig. 7 shows the UV-vis absorption spectrum of the compounds **11a-m** in chloroform solution at 3.3×10^{-2} mM concentration.

Compounds **11a-m** with chalcone linkages showed two broad absorption bands at 264 and 358 nm. Absorption wavelengths λmax are quite similar for all the compounds and no any significant change is observed which may be due to similar molecular structure. There is only change in length of terminal alkoxy chain hence there is no major shift in absorption peak for compounds **11a-m**. In absorption spectra of compounds **11a-m**, the characteristic peak was observed at 264 nm and at 358 nm corresponding to π-π* transition of coumarin [26,27]. As mentioned in literature [26] it seems the n-π*transition has merged with π-π* transition. The absorbance maximum attributed to the π-π* transition of pyrone ring of coumarin nucleus was chosen as excitation wavelength for fluorescence measurements (Fig. 8).

Compounds **11a-k** were excited at λmax of absorbance and their emission spectra were recorded in chloroform at 2.0×10^{-2} mM concentration (Fig. 8). Compound **11a** with methoxy group at terminal position showed good fluorescence having λmax of emission at 421 nm with Stoke shift of 61 nm. On changing alkyl chain to ethoxy in compound **11b**, λmax of emission was observed at 437 nm with bathochromic shift, but intensity of fluorescence was dropped. Similar increase in λmax of emission and drop in fluorescence intensity was observed for compounds **11c-e** with propyl, butyl and pentyl side chains respectively (Fig. 8). Interestingly, compounds **11f-m** showed very poor fluorescence intensity with slight shift in λmax of emission. This drastic drop

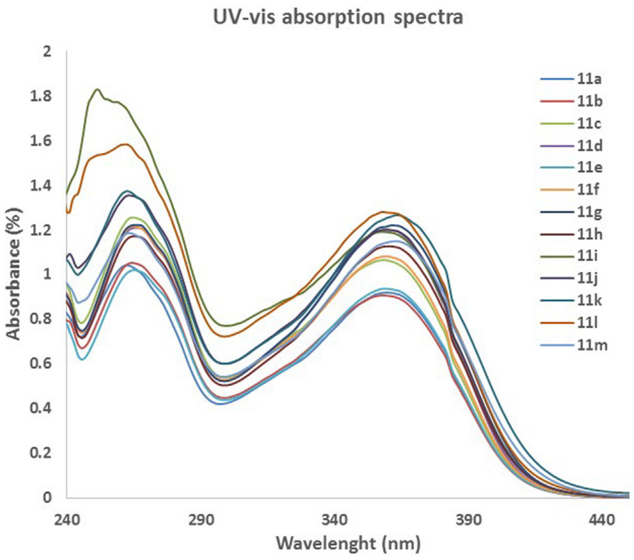

Fig. 7. UV–vis absorption spectra of compounds **11a-m** in $CHCl_3$ at 3.3×10^{-2} mM concentration.

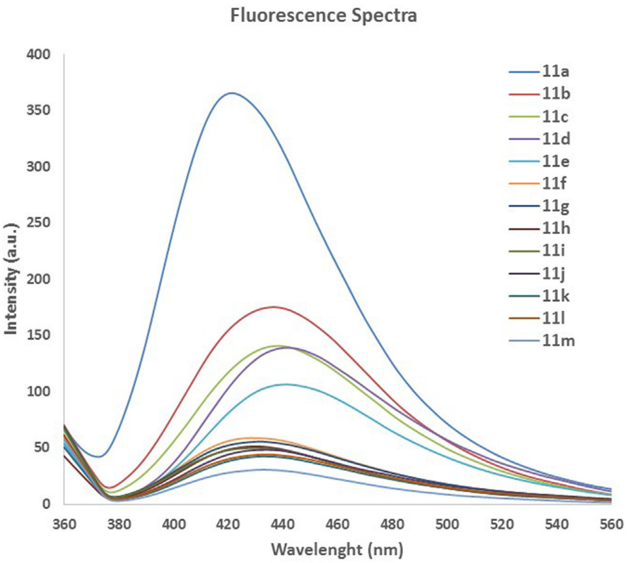

Fig. 8. Fluorescence spectra of compounds **11a-k** in $CHCl_3$ at 2.0 × 10^{-2} mM concentration.

in fluorescence emission of compounds **11a-m** may be due to non-emissive decay caused by various competing processes such as short lifetime of excited molecule, intramolecular or intermolecular relaxation [19,28].

3. Conclusion

Compounds **11a-m** were studied for their mesomorphic properties using polarising optical microscope under both heating and cooling scans at the rate of 10 °C/min. Mesophase transition temperatures were confirmed by DSC thermograms. Compound **11c** showed nematic droplets which was changed to nematic marble texture on cooling. Compound **11d-g** showed nematic marble texture which was changed to nematic schlieren texture on cooling. Interestingly higher chain analogues from C8 onwards did not show any mesophase transitions during heating and cooling cycles. Compound **11h-m** showed direct crystallization during cooling cycle without any mesophase. Thus, bis esters containing chalcone moiety with coumarin heterocycle having lower flexible alkoxy chains showed mesogenic properties, but its higher chain analogues failed to show any liquid crystalline properties. Thus, mesomorphic behaviour of bis ester coumarin derivatives containing chalcone linkage has been widely affected on varying flexible terminal alkyl chains on both ends. Compounds were also studied for their photophysical properties. Compound **11a** with methoxy chain showed very good fluorescence as compared to higher chain length analogues this may be due to the non-emissive decay in molecule with higher chain lengths.

4. Experimental

4.1. Methods and materials

Reagent grade chemicals and solvents were purchased from commercial supplier and used after purification. Thin-layer chromatography was performed on silica gel F254 plates (Merck & Co., Kenilworth, NJ, USA). Acme's silica gel (60–120 mesh) was used for column chromatographic purification. All reactions were carried out in normal atmosphere. Melting points are uncorrected and were measured in open capillary tubes. IR spectra were recorded as KBr pellets on Bruker spectrometer.^{1}H NMR and^{13}C-NMR spectral data were recorded on Avance Bruker Neo 400/500 spectrometer (400/500 MHz) with $CDCl_3$ or DMSO d_6 as solvent and J values are in Hz. Thermograms were calculated by DSC (DSC-822, Mettler Toledo having Stare software) in heating and cooling cycle at the rate of 10 °C/min. Liquid crystal properties were studied using Polarizing Optical Microscope -LEICA DM 2500P, CAMERA- LEICA-DFC 295 and Heating Pod- LINKA 19. UV-Vis spectra were recorded on PerkinElmer Lambda- 35 dual beam UV-Vis spectrophotometer. Fluorescence spectra were recorded on JASCO FP-6300 fluorescence spectrophotometer.

4.2. Synthesis

4.2.1. Synthesis of 4-n-alkyloxybenzoic acid (7b-m)

To a solution of 4-hydroxy benzoic acid (3.5 g, 0.03 mmol, 1 eq) in methanol (25 mL) was added KOH (3.5 g, 0.06 mmol, 2.5 eq) and stirred for 8–10 min. To this solition, alkyl bromide (0.03 mmol, 1.2 eq) was added and resulting mixture was refluxed at 64–66 °C for 6–7 h. During this time, solid was separated out in reaction mixture. To this reaction mixture, 20% aq solution of KOH (5 mL) was added and refluxed for another 2 h to give clear solution. The reaction mixture was allowed to cool down to room temperature and was acidified by 10% HCl solution (25 mL) followed by addition of ice-cold water to give solid. The solid separated out was filtered, dried and recrystallized from absolute ethanol to give pure compound **7b-m**.

4.2.2. Synthesis of 3-acetyl-7-hydroxy coumarin (8)

To a solution of resorcaldehyde (15.0 g, 0.108 mol, 1.0 eq) in ethanol (50 mL) was added ethyl acetoacetate (13.62 mL, 0.108 mol, 1.0 eq) followed by catalytic amount of piperidine (0.1 mL). The resulting mixture was refluxed for 18 h. The completion of reaction was checked by TLC. After completion of reaction, reaction mixture was allowed to cool down to room temperature and concentrated on a rotavapor. The viscous liquid obtained was poured into ice cold water to give solid. The solid obtained was filtered, washed with water, dried and recrystallized from ethanol to give compound **8** as green crystals. Yield: 95%; M.P : 236–238 °C (Lit^1 M.P. 240 °C).

4.2.3. (E)-7-hydroxy-3-(3-(4-hydroxyphenyl)acryloyl)–2H-chromen-2-one (10)

To a solution of compound **8** (1.02 g, 5.0 mmol) in ethanol (50 mL) was added 4-hydroxy benzaldehyde **9** (0.61 g, 5.0 mmol) and stirred for 10–15 min. To this mixture, catalytic amount of pyrrolidine and acetic acid were added and resulting mixture was refluxed at 78–80 °C for 36 h. The completion of reaction was checked by TLC. After completion of reaction, the reaction mixture was allowed to cool to room temperature, concentrated on rotavapor and poured into ice cold water to give brown solid. The crude product was filtered, washed with water, and dried. The crude compound was purified by column chromatography using pet ether:ethyl acetate (7:3) to give pure compound **10** as bright orange solid. Yield: 48%; M.P: >260 °C; ^{1}H NMR (400 MHz, DMSO d_6): δ 6.7 (d, 1H), 6.82–6.86 (m, 3H), 7.58 (d, J = 8.4 Hz, 2H), 7.62 (d, J = 15.6 Hz, 1H), 7.62 (d, J = 15.6 Hz, 1H), 7.77 (d, J = 8.4 Hz, 1H), 8.61 (s, 1H), 10.16 (s, 1H); ^{13}C NMR (100 MHz, DMSO d_6): δ ppm 102.28, 111.55, 114.60, 116.44, 120.81, 121.68, 126.13, 131.21, 132.79, 144.18, 148.37, 157.47, 159.56, 160.69, 164.35, 186.58.

4.2.4. Synthesis of bis-ester coumarin chalcone derivatives 11a-m

To the solution of 4-alkoxy benzoic acid **8a-m** (1.30 mmol, 2.0 eq) in DCM (25 mL) was added EDC (0.37 g, 1.95 mmol, 3.0 eq), HOBt (0.17 g, 1.30 mmol, 2.0 eq) followed by addition of TEA (0.27 mL, 1.95 mmol, 3.0 eq). The resulting solution was stirred at 0–5 °C for 10–15 min. To this cold reaction mixture, compound **10**(0.20 g, 0.65 mmol, 1.0 eq) was added and stirred for 30 min at 0–5 °C and then at room temperature for 20 h. The completion of reaction was checked by TLC. After completion of reaction, the reaction mixture was diluted with water (30 mL) and extracted with DCM (3 × 20 mL). The organic layer was separated, washed with water (20 mL), brine solution (20 mL), dried over anhydrous Na_2SO_4, filtered and concentrated on a rotavapor to give residue. The residue was scratched in methanol, filtered and dried to give compound **11a-m** as yellow solid.

4.2.4.1. (E)-4-(3-(7-((4-Methoxybenzoyl)oxy)-2-oxo-2H-chromen-3-yl)-3-oxoprop-1-en-1-yl)phenyl 4-methoxybenzoate (11a). Yellow solid, Yield: 84%; M.P: 188–190 °C; IR (KBr): 2934, 2840, 1730, 1661, 1608, 1578, 1556, 1511, 1460, 1419, 1366, 1327, 1261, 1165, 1150, 1063, 1026, 863, 844, 758 cm^{-1}; ^{1}H NMR (400 MHz, $CDCl_3$): δ 3.92 (s, 3H), 3.93 (s, 3H), 7.01 (d, J = 8.8 Hz, 2H), 7.02 (d, J = 8.8 Hz, 2H), 7.26–7.34 (m, 4H), 7.73–7.77 (m, 3H), 7.90 (d, J = 16.0 Hz, 1H), 7.96 (d, J = 16.0 Hz, 1H), 8.17 (d, J = 8.4 Hz, 4H), 8.63 (s, 1H); ^{13}C NMR (100 MHz, $CDCl_3$): δ ppm 55.64, 55.68, 110.41, 113.92, 114.09, 116.24, 119.48, 120.67, 121.42, 122.45, 123.84, 124.23, 130.19, 130.97, 132.39, 132.42, 132.61, 144.16, 147.86, 153.00, 155.76, 156.08, 159.18, 163.95, 164.05, 164.41, 164.59, 186.20; Anal. Calc. for $C_{34}H_{24}O_9$; C, 70.83; H, 4.20; found: C, 70.86; H, 4.32%.

4.2.4.2. (E)-4-(3-(7-((4-Ethoxybenzoyl)oxy)-2-oxo-2H-chromen-3-yl)-3-oxoprop-1-en-1-yl)phenyl 4-ethoxybenzoate (11b). Yellow solid, Yield: 80%; M.P: 182–184 °C; IR (KBr): 3086, 3062, 2980, 2931, 1728, 1659, 1604, 1577, 1551, 1508, 1421, 1351, 1252, 1164, 1125, 1061, 920, 870, 848, 760 cm^{-1}; ^{1}H NMR (400 MHz, $CDCl_3$): δ 1.46–1.50 (m, 6H), 4.12–4.18 (m, 4H), 6.98–7.01 (m, 4H), 7.26–7.34 (m, 4H), 7.73–7.77 (m, 3H), (t, J = 7.2 Hz, 4H), 7.28–7.34 (m, 4H), 7.74–7.78 (m, 3H), 7.99 (d, J = 15.6 Hz,1H), 7.96 (d, J = 15.6 Hz, 1H), 8.5 (d, J = 8.0 Hz, 4H), 8.63 (s,1H); ^{13}C NMR (100 MHz, $CDCl_3$): δ ppm 14.67, 14.69, 63.86, 63.95, 110.40, 114.33, 114.49, 116.21, 119.47, 120.43, 121.19, 122.44, 123.84, 124.22, 130.17, 130.95, 132.37, 132.41, 132.60, 144.14, 147.84, 153.03, 155.80, 156.09, 159.16, 163.49, 163.85, 163.96, 164.60, 186.18; Anal. Calc. for $C_{36}H_{28}O_9$; C, 71.52; H, 4.67; found: C, 71.68; H, 4.87%.

4.2.4.3. (E)-4-(3-(7-((4-(Propoxy)benzoyl)oxy)-2-oxo-2H-chromen-3-yl)-3-oxoprop-1-en-1-yl)phenyl 4-(propoxy)benzoate (11c). Yellow solid, Yield: 72%; M.P: 174–176 °C; IR (KBr): 3075, 3059, 2965, 2937, 2877, 1728, 1659, 1603, 1577, 1549, 1508, 1421, 1352, 1324, 1316, 1255, 1227, 1163, 1123, 1061, 991, 868, 844, 760 cm^{-1}; ^{1}H NMR (400 MHz, $CDCl_3$): δ 1.09 (t, J = 7.2 Hz, 6H), 1.87–1.88 (m, 4H), 4.03–4.04 (m, 4H), 7.01 (t, J = 7.2 Hz, 4H), 7.28–7.34 (m, 4H), 7.74–7.78 (m, 3H), 7.91 (d, J = 15.6 Hz,1H), 7.97 (d, J = 15.6 Hz, 1H), 8.16 (d, J = 8.0 Hz, 4H), 8.65 (s,1H); ^{13}C NMR (100 MHz, $CDCl_3$): δ ppm10.50, 22.44, 22.45, 69.80, 69.87, 110.40, 114.35, 114.51, 116.20, 119.47, 120.36, 121.13, 122.44, 123.84, 124.20, 130.17, 130.95, 132.39, 132.58, 144.13, 147.84, 153.03, 155.80, 156.08, 159.16, 163.69, 163.97, 164.05, 164.61, 186.18; Anal. Calc. for $C_{38}H_{32}O_9$; C, 72.14; H, 5.10; found: C, 72.328; H, 5.23%.

4.2.4.4. (E)-4-(3-(7-((4-(Butoxy)benzoyl)oxy)-2-oxo-2H-chromen-3-yl)-3-oxoprop-1-en-1-yl)phenyl 4-(butoxy)benzoate (11d). Yellow solid, Yield: 74%; M.P: 180–182 °C; IR (KBr): 3082, 3058, 2956, 2934, 2870, 1727, 1659, 1603, 1577, 1507, 1420, 1351, 1319, 1257, 1226, 1166, 1148, 1060, 1003, 870, 846, 759, 712 cm^{-1}; ^{1}H NMR (400 MHz, $CDCl_3$): δ1.02 (t, J = 7.2 Hz, 6H), 1.49–1.58 (m, 4H), 1.80–1.87 (m, 4H), 4.06–4.10 (m, 4H), 7.00 (d, J = 8.4 Hz, 2H), 7.01 (d, J = 8.4 Hz, 2H), 7.26–7.34 (m, 4H), 7.74–7.78 (m, 3H), 7.90 (d, J = 16.0 Hz, 1H), 7.97 (d, J = 16.0 Hz, 1H), 8.16 (d, J = 8.8 Hz, 4H), 8.64 (s, 1H); ^{13}C NMR (125 MHz, $CDCl_3$): δ ppm 13.85, 19.21, 31.11, 31.13, 68.05, 68.13, 110.38, 114.36, 114.52, 116.21, 119.44, 120.40, 121.16, 122.43, 123.87, 124.22, 130.15, 130.93, 132.38, 132.57, 144.09, 147.78, 153.06, 155.82, 156.09, 159.13, 163.71, 163.94, 164.07, 164.57, 186.13; Anal. Calc. for $C_{40}H_{36}O_9$; C, 72.71; H, 5.49; found: C, 72.87; H, 5.61%.

4.2.4.5. (E)-4-(3-(7-((4-(Pentyloxy)benzoyl)oxy)-2-oxo-2H-chromen-3-yl)-3-oxoprop-1-en-1-yl)phenyl 4-(pentyloxy)benzoate (11e). Yellow solid, Yield: 91%; M.P: 168–170 °C; IR (KBr): 3077, 2934, 2867, 1727, 1662, 1607, 1579, 1508, 1468, 1419, 1320, 1257, 1232, 1167, 1145, 1063, 1006, 988, 842, 759 cm^{-1}; ^{1}H NMR (400 MHz, $CDCl_3$): δ 0.97 (t, J = 6.8 Hz, 6H), 1.39–1.50 (m, 8H), 1.82–1.88 (m, 4H), 4.05–4.09 (m, 4H), 6.99 (d, J = 8.8 Hz, 2H), 7.01 (d, J = 8.8 Hz, 2H), 7.26–7.34 (m, 4H), 7.74–7.77 (m, 3H), 7.90 (d, J = 16.0 Hz, 1H), 7.97 (d, J = 16.0 Hz, 1H), 8.17 (d, J = 8.4 Hz, 4H), 8.64 (s, 1H); ^{13}C NMR (125 MHz, $CDCl_3$): δ ppm 14.03, 22.45, 28.13, 28.77, 28.79, 68.35, 68.43, 110.38, 114.36, 114.52, 116.20, 119.44, 120.39, 121.15, 122.43, 123.88, 124.22, 130.14, 130.93, 132.38, 132.57, 144.09, 147.78, 153.06, 155.82, 156.09, 159.13, 163.71, 163.95, 164.06, 164.59, 186.15; Anal. Calc. for $C_{42}H_{40}O_9$; C, 73.24; H, 5.85; found: C, 73.38; H, 5.98%.

4.2.4.6. (E)-4-(3-(7-((4-(Hexyloxy)benzoyl)oxy)-2-oxo-2H-chromen-3-yl)-3-oxoprop-1-en-1-yl)phenyl 4-(hexyloxy)benzoate (11f). Yellow solid, Yield: 89%; M.P: 166–168 °C; IR (KBr): 2932, 2866, 1727, 1660, 1606, 1578, 1508, 1468, 1420, 1319, 1255, 1231, 1167, 1147, 1063, 1001, 868, 758 cm^{-1}; ^{1}H NMR (400 MHz, $CDCl_3$): δ 0.93 (t, J = 6.8 Hz, 6H), 1.37–1.38 (m, 8H), 1.48–1.52 (m, 4H), 1.82–1.86 (m, 4H), 4.04–4.08 (m, 4H), 6.99 (d, J = 8.8 Hz, 2H), 7.01 (d, J = 8.8 Hz, 2H), 7.26–7.34 (m, 4H), 7.73–7.77 (m, 3H), 7.90 (d, J = 15.6 Hz, 1H), 7.96 (d, J = 15.6 Hz, 1H), 8.15 (d, J = 8.4 Hz, 4H), 8.64 (s,1H); ^{13}C NMR (125 MHz, $CDCl_3$): δ ppm 14.05, 22.60, 25.66, 29.04, 29.06, 31.55, 68.37, 68.45, 110.38, 114.37, 114.52, 116.21, 119.44, 120.39, 121.15, 122.44, 123.88, 124.23, 130.15, 130.93, 132.38, 132.57, 144.10, 147.78, 153.06, 155.82, 156.09, 159.14, 163.71, 163.95, 164.07, 164.59, 186.15; Anal. Calc. for $C_{44}H_{44}O_9$; C, 73.73; H, 6.19; found: C, 73.88; H, 6.33%.

4.2.4.7. (E)-4-(3-(7-((4-(Heptyloxy)benzoyl)oxy)-2-oxo-2H-chromen-3-yl)-3-oxoprop-1-en-1-yl)phenyl 4-(heptyloxy)benzoate (11g). Yellow solid, Yield: 70%; M.P: 170–172 °C; IR (KBr): 2925, 2859, 1727, 1661, 1607, 1506, 1463, 1420, 1261, 1222, 1163, 1066, 1003, 840, 813, 761 cm^{-1}; ^{1}H NMR (400 MHz, $CDCl_3$): δ 0.92 (t, J = 6.8 Hz, 6H), 1.34–1.41 (m, 12H), 1.46–1.49 (m, 4H), 1.81–1.86 (m, 4H), 4.05–4.09 (m, 4H), 6.99 (d, J = 8.4 Hz, 2H), 7.01 (d, J = 8.8 Hz, 2H), 7.24–7.34 (m, 4H), 7.69–7.80 (m, 3H), 7.91 (d, J = 15.6 Hz,1H), 7.96 (d, J = 15.6 Hz,1H), 8.16 (d, J = 8.4 Hz, 4H), 8.64 (s, 1H); ^{13}C NMR (125 MHz, $CDCl_3$): δ ppm 14.12, 22.63, 25.96, 29.05, 29.09, 29.11, 31.77, 68.37, 68.45, 110.38, 114.37, 114.53, 116.20, 119.45, 120.37, 121.12, 122.44, 123.87, 124.19, 129.98, 130.16, 130.94, 132.39, 132.57, 144.11, 147.81, 153.05, 155.83, 156.08, 159.16, 163.73, 163.96, 164.08, 164.65, 186.15; Anal. Calc. for $C_{46}H_{48}O_9$; C, 74.17; H, 6.50; found: C, 74.21; H, 6.62%.

4.2.4.8. (E)-4-(3-(7-((4-(Octyloxy)benzoyl)oxy)-2-oxo-2H-chromen-3-yl)-3-oxoprop-1-en-1-yl)phenyl 4-(octyloxy)benzoate (11h). Yellow solid, Yield: 76%; M.P: 164–166 °C; IR (KBr): 2924, 2853, 1726, 1660, 1605, 1578, 1551, 1407, 1419, 1256, 1230, 1167, 1124, 1064, 866, 758, 649 cm^{-1}; ^{1}H NMR (400 MHz, $CDCl_3$): δ 0.91 (t, J = 6.4 Hz, 6H), 1.32–1.37 (m, 16H), 1.46–1.51 (m, 4H), 1.81–1.88 (m, 4H), 4.05–4.09 (m, 4H), 6.99 (d, J = 8.8 Hz, 2H), 7.01 (d, J = 8.8 Hz, 2H), 7.26–7.34 (m, 4H), 7.74–7.78 (m, 3H), 7.90 (d, J = 16.0 Hz, 1H), 7.97 (d, J = 16.0 Hz, 1H), 8.16 (d, *J* = 8.0 Hz, 4H), 8.64 (s,1H); ^{13}C NMR (125 MHz, CDCl$_3$): δ ppm 14.13, 22.68, 25.99, 29.08, 29.10, 29.24, 29.34, 31.82, 68.37, 68.45, 110.37, 114.36, 114.52, 116.20, 119.43, 120.39, 121.15, 122.43, 123.87, 124.21, 130.14, 130.93, 132.38, 132.57, 144.08, 147.78, 153.06, 155.82, 156.09, 159.13, 163.71, 163.94, 164.07, 164.58, 186.12; Anal. Calc. for $C_{48}H_{52}O_9$; C, 74.59; H, 6.18; found: C, 74.78; H, 6.32%.

4.2.4.9. (E)-4-(3-(7-((4-(Decyloxy)benzoyl)oxy)-2-oxo-2H-chromen-3-yl)-3-oxoprop-1-en-1-yl)phenyl 4-(decyloxy)benzoate (11i). Yellow solid, Yield: 64%; M.P: 184–186 °C; IR (KBr): 2924, 2855, 1728, 1661, 1607, 1506, 1465, 1420, 1321, 1261, 1223, 1163, 1065, 1004, 841, 814, 761, 718, 691 cm^{-1}; ^{1}H NMR (400 MHz, CDCl$_3$): δ 0.91 (t, *J* = 6.8 Hz, 6H), 1.30–1.38 (m,24H), 1.46–1.51 (m, 4H), 1.81–1.88 (m, 4H), 4.05–4.09 (m, 4H), 6.98–7.02 (m, 4H), 7.27–7.35 (m,4H), 7.74–7.78 (m,3H), 7.90 (d, *J* = 15.6 Hz, 1H), 7.97 (d, *J* = 15.6 Hz, 1H), 8.16 (d, *J* = 8.4 Hz, 4H), 8.65 (s, 1H); ^{13}C NMR (125 MHz, CDCl$_3$): δ ppm 14.15, 22.70, 25.99, 29.08, 29.10, 29.34, 29.38, 29.57, 31.91, 68.37, 68.45, 110.39, 114.37, 114.53, 116.21, 119.45, 120.38, 121.13, 122.44, 123.87, 124.22, 129.99, 130.16, 130.93, 132.39, 132.57, 144.12, 147.81, 153.06, 155.83, 156.09, 159.16, 163.72, 163.96, 164.08, 164.63, 186.16; Anal. Calc. for $C_{52}H_{60}O_9$; C, 75.34; H, 7.30; found: C, 75.49; H, 7.44%.

4.2.4.10. (E)-4-(3-(7-((4-(Dodecyloxy)benzoyl)oxy)-2-oxo-2H-chromen-3-yl)-3-oxoprop-1-en-1-yl)phenyl 4-(dodecyloxy)benzoate (11j). Yellow solid, Yield: 79%; M.P: 182–184 °C; IR (KBr): 2920, 2850, 1729, 1660, 1605, 1577, 1507, 1469, 1419, 1350, 1317, 1257, 1214, 1169, 1148, 1066, 1003, 842, 759 cm^{-1}; ^{1}H NMR (400 MHz, CDCl$_3$): δ 0.90 (t, *J* = 6.8 Hz, 6H), 1.29 (brs, 32H), 1.46–1.49 (m, 4H), 1.83–1.86 (m,4H), 4.05–4.09 (m, 4H), 6.99 (d, *J* = 8.8 Hz,2H), 7.01 (d, *J* = 8.8 Hz, 2H), 7.27–7.35 (m, 4H), 7.74–7.78 (m, 3H), 7.90 (d, *J* = 15.6 Hz, 1H), 7.97 (d, *J* = 15.6 Hz, 1H), 8.16 (d, *J* = 8.0 Hz, 4H), 8.64 (s, 1H); ^{13}C NMR (125 MHz, CDCl$_3$): δ ppm 14.15, 22.71, 25.99, 29.08, 29.10, 29.37, 29.57, 29.61, 29.65, 29.67, 31.94, 68.37, 68.45, 110.38, 114.37, 114.53, 116.21, 119.43, 120.40, 121.66, 122.43, 123.88, 124.24, 130.14, 130.97, 132.38, 132.57, 144.10, 147.76, 153.06, 155.83, 156.10, 159.13, 163.71, 163.94, 164.08, 164.58, 186.14; Anal. Calc. for $C_{56}H_{68}O_9$; C, 75.99; H, 7.74; found: C, 76.09; H, 7.85%.

4.2.4.11. (E)-4-(3-(7-((4-(Tetradecyloxy)benzoyl)oxy)-2-oxo-2H-chromen-3-yl)-3-oxoprop-1-en-1-yl)phenyl 4-(tetradecyloxy)benzoate (11k). Yellow solid, Yield: 75%; M.P: 156–158 °C; IR (KBr): 2920,2852,1728,1662,1609,1577,1509,1468,1332,1258,1165,1066, 835,769 cm^{-1}; ^{1}H NMR (400 MHz, CDCl$_3$): δ 0.90 (t, *J* = 6.8 Hz, 6H), 1.28 (brs, 40H), 1.46–1.51 (m, 4H), 1.81–1.86 (m, 4H), 4.05–4.09 (m, 4H), 6.99 (d, *J* = 8.8 Hz, 2H), 7.01 (d, *J* = 8.8 Hz, 2H), 7.27–7.34 (m, 4H), 7.90 (d, *J* = 15.6 Hz, 1H), 7.97 (d, *J* = 15.6 Hz, 1H), 8.16 (d, *J* = 8.8 Hz, 4H), 8.65 (s,1H); ^{13}C NMR (125 MHz, CDCl$_3$): δ ppm 14.18, 22.72, 25.99, 29.07, 29.09, 29.33, 29.39, 29.58, 29.62, 29.68, 31.95, 68.36, 68.44, 110.40, 114.00, 114.34, 114.50, 116.20, 119.48, 120.33, 121.08, 122.45, 123.82, 124.19, 130.18, 130.95, 131.52, 132.39, 132.58, 144.16, 147.86, 153.03, 155.80, 156.07, 159.18, 163.98, 164.06, 164.64, 186.19; Anal. Calc. for $C_{60}H_{76}O_9$; C, 76.56; H, 8.14; found: C, 76.68; H, 8.26%.

4.2.4.12. (E)-4-(3-(7-((4-(Hexadecyloxy)benzoyl)oxy)-2-oxo-2H-chromen-3-yl)-3-oxoprop-1-en-1-yl)phenyl 4-(hexadecyloxy)benzoate (11l). Yellow solid, Yield: 65%; M.P: 154–156 °C; IR (KBr): 2918, 2851, 1725, 1660, 1610, 1577, 1507, 1469, 1420, 1320, 1259, 1169, 1073, 835, 764 cm^{-1}; ^{1}H NMR (400 MHz, CDCl$_3$): δ 0.89 (t, *J* = 6.8 Hz, 6H), 1.27 (brs, 48H), 1.47–1.49 (m, 4H), 1.82–1.85 (m, 4H), 4.04–4.08 (m, 4H), 6.99 (d, *J* = 8.8 Hz,2H), 7.01 (d, *J* = 8.4 Hz,2H), 7.27–7.34 (m, 4H), 7.74–7.77 (m, 3H), 7.90 (d, *J* = 15.8 Hz, 1H), 7.97 (d, *J* = 15.8 Hz, 1H), 8.15 (d, *J* = 8.0 Hz, 4H), 8.64 (s, 1H); ^{13}C NMR (125 MHz, CDCl$_3$): δ ppm14.18, 22.73, 25.99, 29.08, 29.10, 29.40, 29.59, 29.62, 29.69, 29.72, 31.95, 68.36, 68.44, 110.40, 114.35, 114.50, 116.21, 1119.48, 120.33, 121.09, 122.45, 128.83, 124.20, 130.18, 130.95, 132.39, 132.58, 144.15, 147.86, 153.04, 155.81, 156.08, 159.17, 163.70, 163.98, 164.06, 164.63, 186.19; Anal. Calc. for $C_{64}H_{84}O_9$; C, 77.07; H, 8.49; found: C, 77.19; H, 8.63%.

4.2.4.13. (E)-4-(3-(7-((4-(Octadecyloxy)benzoyl)oxy)-2-oxo-2H-chromen-3-yl)-3-oxoprop-1-en-1-yl)phenyl 4-(octadecyloxy)benzoate (11m). Yellow solid, Yield: 63%; M.P: 166–168 °C; IR (KBr): 3436, 2918, 2851, 1728, 1663, 1608, 1579, 1510, 1470, 1281, 1257, 1170, 1151, 1071, 844, 832, 759 cm^{-1}; ^{1}H NMR (400 MHz, CDCl$_3$): δ 0.90 (t, *J* = 7.2 Hz, 6H), 1.27 (brs, 56H), 1.46–1.50 (m, 4H), 1.83–1.86 (m, 4H), 4.05–4.09 (m, 4H), 6.99 (d, *J* = 8.8 Hz, 2H), 7.01 (d, *J* = 8.4 Hz, 2H), 7.25–7.35 (m, 4H), 7.75 (d, *J* = 8.4 Hz, 1H), 7.76 (d, *J* = 8.4 Hz, 1H), 7.89–8.01 (m, 2H), 8.16 (d, *J* = 8.4 Hz, 4H), 8.65 (s, 1H); ^{13}C NMR (125 MHz, CDCl$_3$): δ ppm 14.17, 22.72, 25.99, 29.08, 29.39, 29.59, 29.62, 29.69, 29.73, 31.95, 68.35, 68.43, 110.39, 113.99, 114.34, 114.50, 116.20, 119.47, 120.33, 121.09, 122.44, 123.82, 124.18, 130.17, 132.38, 132.57, 144.15, 147.85, 153.03, 155.80, 156.07, 159.16, 163.69, 163.97, 164.05, 164.62, 186.17; Anal. Calc. for $C_{68}H_{92}O_9$; C, 77.53; H, 8.80; found: C, 77.78; H, 8.97%.

Declaration of Competing Interest

The authors declare that they have no known competing financial interests or personal relationships that could have appeared to influence the work reported in this paper.

Acknowledgements

One of the authors (RS) is thankful to Department of Science & Technology, Government of India for financial support vide reference no. SR/WOS-A/CS-9/2018 under Women Scientist Scheme to carry out this work. Authors are also thankful to The Head, Department of Chemistry, Faculty of Science, The M. S. University of Baroda for providing laboratory facilities, DST-FIST for providing NMR and POM facilities.

Appendix A. Supplementary data

Supplementary data to this article can be found online at https://doi.org/10.1016/j.molliq.2021.116178.

References

[1] M. Sato, R. Ishii, S. Nakashima, K. Yonetake, J. Kido, Liq. Cryst. 28 (2001) 1211–1214, https://doi.org/10.1080/02678290110051594.

[2] H. Gallardo, G. Conte, P.A. Tuzimoto, B. Behramand, F. Molin, J. Eccher, I.H. Bechtold, Liq. Cryst. 39 (2012) 1099–1111, https://doi.org/10.1080/02678292.2012.698313.

[3] J. Han, X. Wang, X.-Y. Chang, L.-R. Zhu, Liq. Cryst. 39 (2012) 669–674, https://doi.org/10.1080/02678292.2012.671966.

[4] C. Chai, Q. Yang, X. Fan, X. Chen, Z. Shen, Q. Zhou, Liq. Cryst. 35 (2008) 133–141, https://doi.org/10.1080/02678290701793881.

[5] D. Devadiga, T.N. Ahipa, RSC Adv. 9 (2019) 23161–23228, https://doi.org/10.1039/C9RA04389F.

[6] W. Weissflog, D. Demus, Mol. Cryst. Liq. Cryst. 129 (1985) 235–243, https://doi.org/10.1080/15421408408084178.

[7] G.W. Gray, Molecular Structure and the Properties of Liquid Crystals, Academic press, Cambridge, MA, USA, 1962.

[8] W.H. De Jeu, Physical Properties of Liquid Crystalline Materials, vol. 1, CRC Press, Boca Raton, FL, USA, 1980.

[9] B.D. Wagner, Molecules 14 (2009) 210–237, https://doi.org/10.3390/molecules14010210.

[10] Z.-S. Wang, K. Hara, Y. Dan-oh, C. Kasada, A. Shinpo, S. Suga, H. Arakawa, H. Sugihara, J. Phys. Chem. B 109 (2005) 3907–3914, https://doi.org/10.1021/jp044851v.

[11] C.-T. Chen, C.-L. Chiang, Y.-C. Lin, L.-H. Chan, C.-H. Huang, Z.-W. Tsai, C.-T. Chen, Org. Lett. 5 (2003) 1261–1264, https://doi.org/10.1021/ol034268h.

[12] G. Jones II, W.R. Jackson, C.Y. Choi, W.R. Bergmark, J. Phys. Chem. 89 (1985) 294–300, https://doi.org/10.1021/j100248a024.

[13] D. Gindre, K. Iliopoulos, O. Krupka, M. Evrard, E. Champigny, M. Sallé, Molecules 21 (2016) 147, https://doi.org/10.3390/molecules21020147.

[14] S.R. Trenor, A.R. Shultz, B.J. Love, T.E. Long, Coumarins in polymers: from light harvesting to photo-cross-linkable tissue scaffolds, Chem. Rev. 104 (2004) 3059–3078, https://doi.org/10.1021/cr030037c.

[15] Y. Li, X. Chen, P. Chen, Z. An, J. Li, Liq. Cryst. 37 (2010) 1549–1557, https://doi.org/10.1080/02678292.2010.527019.

[16] A.A. Merlo, A. Tavares, S. Khan, M.J. Leite Santos, S.R. Teixeria, *Liq. Cryst.* 45 (2018) 310–322, https://doi.org/10.1080/02678292.2017.1324644.

[17] Y. Tian, E. Akiyama, Y. Nagase, J. Mater. Chem. 13 (2003) 1253–1258, https://doi.org/10.1039/B302857G.

[18] Y. Morita, H. Ushijima, K. Era, K. Kasatani, H. Okamoto, Mol. Cryst. Liq. Cryst. 494 (2008) 282–292, https://doi.org/10.1080/15421400802430000.

[19] H.T. Srinivasa, H.N. Harishkumar, B.S. Palakshamurthy, J. Mol. Struct. 1131 (2017) 97–102, https://doi.org/10.1016/j.molstruc.2016.11.047.

[20] H.T. Srinivasa, B.S. Palakshamurthy, A.T. Mohammad, J. Mol. Struct. 1155 (2018) 513–519, https://doi.org/10.1016/j.molstruc.2017.11.055.

[21] M. Hagar, H.A. Ahmed, O.A. Alhaddadd, Crystals 8 (2018) 359, https://doi.org/10.3390/cryst8090359.

[22] A.T. Mohammad, M.H. Al-Mohammedi, M.Z. Ghdhayeb, S.M. Husain Al-Majidi, *Liq. Cryst.* 47 (2020) 414–422, https://doi.org/10.1080/02678292.2019.1655806.

[23] A.T. Mohammad, M.H. Al-Mohammedi, H.T. Srinivasa, W.A. Ameen, J. Mol. Liq. 314 (2020), https://doi.org/10.1016/j.molliq.2020.113782 113782.

[24] E. Madiahlagan, B.N. Sunil, Z. Ngaini, G. Hegde, J. Mol. Liq. 292 (2019), https://doi.org/10.1016/j.molliq.2019.111328 111328.

[25] S.D. Durgpal, R. Soni, S.S. Soman, A.K. Prajapati, J. Mol. Liq. 297 (2019), https://doi.org/10.1016/j.molliq.2019.111920 111920.

[26] R.H. Abu-Eittah, B.A.H. El-Tawil, Can. J. Chem. 63 (1985) 1173–1179, https://doi.org/10.1139/v85-200.

[27] J. Donovalová, M. Cigáň, H. Stankovičová, J. Gašpar, M. Danko, A. Gáplovský, P. Hrdlovič, Molecules 17 (2012) 3259–3276, https://doi.org/10.3390/molecules17033259.

[28] K. Muhammad, K. Khawar Rauf, M. Nawaz Tahir, S. Hameed, *Mol. Cryst. Liq. Cryst.* 650 (2017) 32–45, https://doi.org/10.1080/15421406.2017.1328215.